9-1-2019

Exome sequencing of ABCB5 identifies recurrent melanoma mutations that result in increased proliferative and invasive capacities

Géraldine Sana

James P Madigan

Jared J Gartner

Marie Fourrez

Jimmy Lin

See next page for additional authors

Authors

Géraldine Sana, James P Madigan, Jared J Gartner, Marie Fourrez, Jimmy Lin, Nouar Qutob, Jitendra Narayan, Suneet Shukla, Suresh V Ambudkar, Di Xia, Steven A Rosenberg, Michael M Gottesman, Yardena Samuels, and Jean-Pierre Gillet

Exome Sequencing of ABCB5 Identifies Recurrent Melanoma Mutations that Result in Increased Proliferative and Invasive Capacities

JID Open

Géraldine Sana[1], James P. Madigan[2], Jared J. Gartner[3], Marie Fourrez[1], Jimmy Lin[4], Nouar Qutob[5], Jitendra Narayan[6], Suneet Shukla[2], Suresh V. Ambudkar[2], Di Xia[2], Steven A. Rosenberg[7], Michael M. Gottesman[2], Yardena Samuels[3,5] and Jean-Pierre Gillet[1]

ABCB5 is an ABC transporter that was shown to confer low-level multidrug resistance in cancer. In this study, we show that ABCB5 was mutated in 13.75% of the 640 melanoma samples analyzed. Besides nonsense mutations, two mutation hotspots were found in the ABCB5 protein, in the drug-binding pocket and the nucleotide-binding domains. Four mutations, which are representative of the mutation pattern, were selected. ATPase assays showed that these mutations resulted in a decrease in basal ATP hydrolysis by ABCB5. To select informative melanoma cell lines, mutational profiles of the clinical samples were further analyzed. This study showed mutations in the tumor suppressor *CDKN2A* gene and the *NRAS* oncogene in 62.5% and 75%, respectively of the samples that had mutations in the ABCB5 gene. No mutation was found in the tumor suppressor *PTEN* gene, whereas the activating V600E mutation in the BRAF oncogene was found in 25% of the samples with a mutated *ABCB5* gene. Studies in four melanoma cell lines with various genetic backgrounds showed an increase in the proliferation and migration capacity of mutant ABCB5-expressing cells, suggesting that ABCB5 plays a role in the development of melanoma as a tumor suppressor gene.

Journal of Investigative Dermatology (2019) **139,** 1985–1992; doi:10.1016/j.jid.2019.01.036

INTRODUCTION

ABCB5, an ABC transporter closely related to the multidrug transporter ABCB1 (P-glycoprotein), is predominantly expressed in pigment-producing cells. Previous studies have suggested that it is a marker of melanoma-initiating cells (Schatton et al., 2008) and is linked to the development of multidrug resistance in melanoma (Chartrain et al., 2012; Frank et al., 2005). However, those studies were based on the expression of a transcript variant of the ABCB5 gene, namely ABCB5β, which encodes a truncated transporter (Chen et al., 2005; Frank et al., 2003). The functionality of this transporter is controversial and has yet to be directly demonstrated (Kawanobe et al., 2012; Keniya et al., 2014). More recently, the Sugimoto group reported the cloning of a transcript that encodes a typical full ABC transporter, which is composed of two transmembrane and two nucleotide-binding domains (Kawanobe et al., 2012). They showed the involvement of this more typical transporter in resistance to doxorubicin, paclitaxel, and docetaxel (Kawanobe et al., 2012).

ABC transporters have been extensively studied for their role in the mechanisms of multidrug resistance in cancer. Nonetheless, transcriptomic studies carried out to characterize these mechanisms in clinical samples indicated that these transporters may also have a major role in tumor biology (Gillet et al., 2011). Indeed, there is a growing body of evidence that their loss or inhibition have an impact on the malignant potential of cancer cells both in vitro and in vivo (Fletcher et al., 2016). ABCB5 mutations appeared to be common in melanoma (Krauthammer et al., 2015), and we hypothesized that this transporter contributes to the development of melanoma in addition to its role as a drug-efflux transporter.

Here, we report the results of the systematic analysis of the nature and function of mutations in the *ABCB5* gene. Exome sequencing of the *ABCB5* gene was performed in 153 human melanoma samples including matched normal DNA. These data were combined with mutational data from published studies, resulting in a data set generated from 640 human melanoma samples. Mutations were mapped in a three-dimensional predicted model of the protein, and two mutation hotspots in the ABCB5 protein were found. The impact of four mutations, representative of the mutation pattern, was further studied in four melanoma cell lines.

[1]*Laboratory of Molecular Cancer Biology, Molecular Physiology Research Unit (URPHYM), Namur Research Institute for Life Sciences, Faculty of Medicine, Department of Biomedical Sciences, University of Namur, Namur, Belgium;* [2]*Laboratory of Cell Biology, Center for Cancer Research, National Cancer Institute, National Institutes of Health, Bethesda, Maryland, USA;* [3]*Cancer Genetics Branch, National Human Genome Research Institute, National Institutes of Health, Bethesda, Maryland, USA;* [4]*Washington University School of Medicine, Genome Technology Access Center, Genomics and Pathology Services, St. Louis, Missouri, USA;* [5]*Department of Molecular Cell Biology, Weizmann Institute of Science, Rehovot 76100, Israel;* [6]*Laboratory of Evolutionary Genetics and Ecology (LEGE), Faculty of Sciences, Department of Biology, University of Namur, Namur, Belgium; and* [7]*Surgery Branch, National Cancer Institute, National Institutes of Health, Bethesda, Maryland, USA*

Correspondence: Jean-Pierre Gillet, Biology, Molecular Physiology Research Unit, Namur Research Institute for Life Sciences, Faculty of Medicine, Department of Biomedical Sciences, University of Namur, Namur, Belgium. E-mail: jean-pierre.gillet@unamur.be or Michael M. Gottesman, Chief of Laboratory of Cell Biology, National Cancer Institute, 37 Convent Drive, Room 2108, Bethesda, Maryland 20892, USA. E-mail: mgottesman@nih.gov

Abbreviation: shRNA, short hairpin RNA

Received 17 October 2018; revised 19 December 2018; accepted 2 January 2019; accepted manuscript published online 21 March 2019; corrected proof published online 14 May 2019

Table 1. ABCB5 mutations in untreated samples (results of Whole Exome, Whole Genome, and Sanger sequencing in a total of 54 untreated melanoma samples shown)

Sample	Mutation	Mutation Type	Het/ Homo	Type of Screen	SIFT Score	Mutations			CDKN2A Status	PTEN Status	NRAS Status	BRAF Status
						Nonsynonymous	Synonymous	Total				
17T	Q187*	Nonsynonymous	Het	Genome	N/A	438	246	684	WT	WT	Q61K	WT
55T	E520D	Nonsynonymous	Het	Exome	0.21	1,555	835	2,390	WT	WT	WT	WT
44T	R587*	Nonsynonymous	Het	Prevalence	N/A	N/A	N/A	N/A	2:64L>L/P, 83H>H/Y	9:102350G>A (-2 intronic)	Q61K	WT
83T	V827I	Nonsynonymous	Het	Prevalence	1	N/A	N/A	N/A	Deleted	WT	S39F	V600E
12T	I828I	Synonymous	Het	Genome	1	1,061	533	1,594	Deleted	WT	Q61K	WT
83T	S830F	Nonsynonymous	Het	Prevalence	0	N/A	N/A	N/A	Deleted	WT	S39F	V600E
105T	L840L	Synonymous	Het	Prevalence	0.7	N/A	N/A	N/A	Deleted	WT	WT	V600E
32T	S1184P	Nonsynonymous	Het	Genome	0	1091	556	1,647	WT	WT	WT	L597Q
24T	S1091F	Nonsynonymous	Het	Exome	0.01	415	213	628	Deleted	WT	Q61R	WT
55T	Q1098*	Nonsynonymous	Het	Exome	N/A	1,555	835	2,390	WT	WT	WT	WT

Abbreviations: Het, heterogenous; Homo, homogenous; N/A, not applicable; WT, wild type.

RESULTS AND DISCUSSION

Exome sequencing

To identify somatic mutations in ABCB5, we analyzed the coding regions of ABCB5 in 29 melanoma samples and corresponding normal DNA from a previously published study by Gartner et al. (2013). Our initial analysis of these samples showed six mutations, including three nonsynonymous mutations, two nonsense, and one synonymous mutation in five of our 29 samples (17%). The 5:1 nonsynonymous to synonymous ratio (20%) is considerably higher than the ratio predicted for nonselected passenger mutations of 2.5:1 (Sjoblom et al., 2006). Further sequencing of ABCB5 in an additional panel of 25 untreated samples showed four additional mutations in three different samples, including a third nonsense mutation. Taken together, these two analyses showed that ABCB5 contained 10 mutations (eight nonsynonymous) in eight of 54 samples (14.5%; $P < 0.001$) (Table 1). A validation was performed on six of these 10 mutations with digital PCR, which confirmed their presence at the RNA level. Thus, melanoma cells with mutant ABCB5 also contain wild-type mRNAs, resulting in coexpression of mutant and wild-type ABCB5 (data not shown).

We extended the study to an additional cohort containing 99 melanoma samples, which showed 14 additional mutations (nine nonsynonymous and five synonymous). Of these 24 total mutations observed, 17 were nonsynonymous, and four were nonsense mutations affecting 9.8% of our samples (15 of 153).

We also reviewed the mutational data from published studies (Berger et al., 2012; Hodis et al., 2012; Nikolaev et al., 2011; Stark et al., 2011; Wei et al., 2011), which were combined with exome data from The Cancer Genome Atlas, resulting in 487 published melanoma samples. Analysis of ABCB5 in these 487 published melanoma samples showed 85 coding mutations in 73 of 487 samples, or 14.9%. The mutations include 60 nonsynonymous mutations, one splice site mutation, six nonsense mutations, and 18 silent mutations (see Supplementary Table S1 online). In summary, we show that the gene *ABCB5* was mutated in 13.75% of the 640 melanoma samples analyzed.

Effect of the mutations on the transporter activity

Mutations were localized on a two- and three-dimensional predicted models constructed based on the sequence alignment of full-length ABCB5 to mouse ABCB1, for which experimental structures are known (Figure 1a and b) (Esser et al., 2017; Li et al., 2014). Two mutation hotspots were found in the predicted drug binding pocket and the nucleotide binding domains of the ABCB5 protein. The impact of four mutations was further investigated based on their localization in the mutation hotspots and the likely deleterious effect on the transporter activity (Table 1). Besides a nonsense mutation (Q187*), a nonsynonymous mutation was located in the predicted drug binding pocket (S830F), and two were in the second nucleotide binding domain (S1091F, S1184P) (Figure 1c and d).

The effect of the mutations on the transporter activity was assessed by an ATPase assay. All mutants were expressed in High Five insect cells at the same level as wild-type WT protein (Figure 2a). The ATPase assays confirmed that these mutations resulted in a decrease in basal ATP hydrolysis by ABCB5 (Figure 2b). Based on these data, we hypothesized that ABCB5 may play a role in the tumor biology, perhaps as a tumor suppressor.

Impact of the mutations on the proliferation ability of human melanoma cell lines

To explore the deleterious effect of the mutations in vitro, we wanted to determine the genetic background of the ABCB5 mutated melanoma. Further studies on the first set of 54 human melanoma samples analyzed showed mutations in the tumor suppressor *CDKN2A* gene and the *NRAS* oncogene in 62.5% and 75% of the samples, respectively, that had mutations in the *ABCB5* gene. No mutation was found in the tumor suppressor *PTEN* gene, whereas the activating V600E mutation in the BRAF oncogene was found in 25% of the samples with a mutated *ABCB5* gene.

We have chosen the 17T and 63T human melanoma cell lines, both of which harbor the activated mutant NRAS Q61K. The 17T cell line also harbors the heterozygous nonsense mutant ABCB5 Q187*, and WT BRAF, PTEN, and

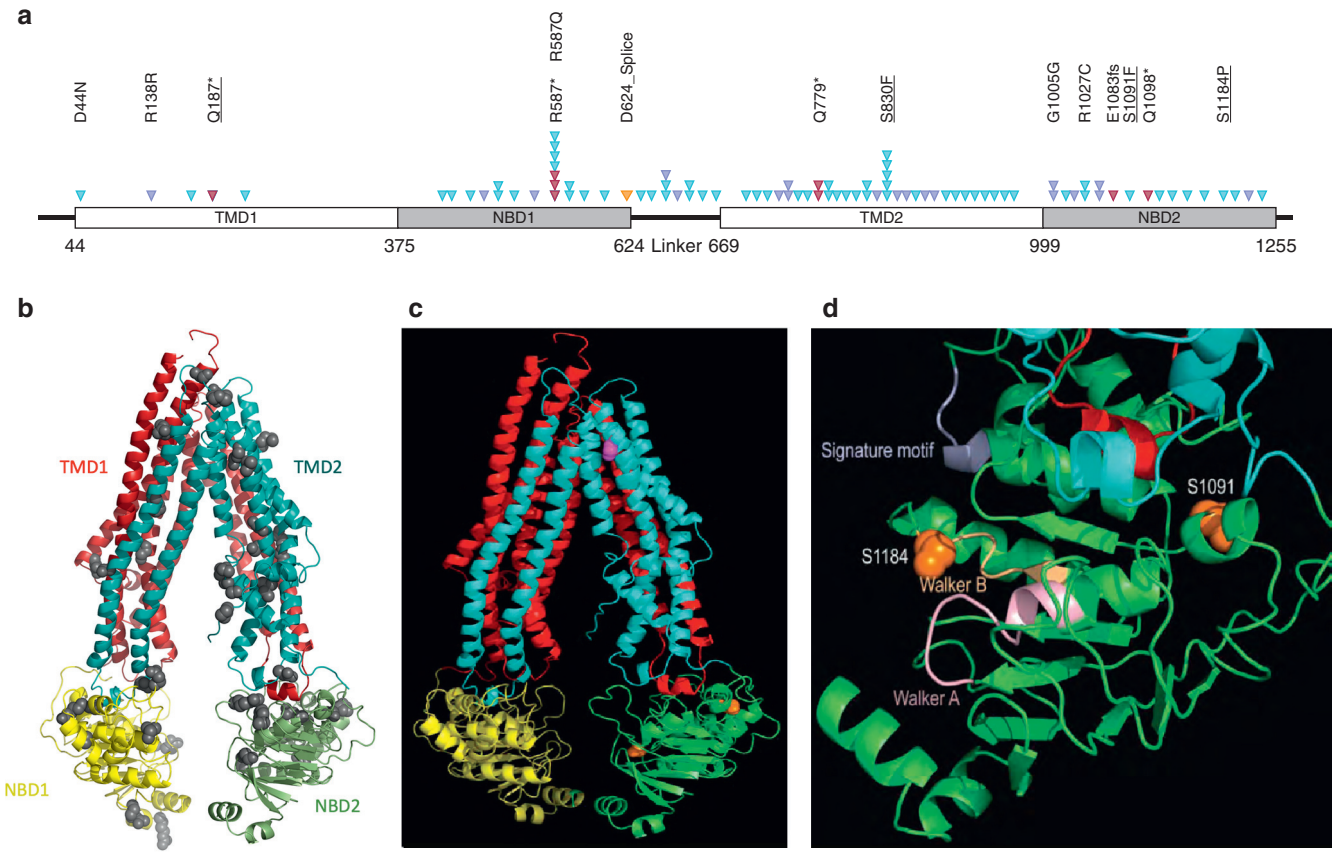

Figure 1. Molecular model of ABCB5. An atomic model of ABCB5 was constructed based on the sequence alignment of full-length ABCB5 to mouse ABCB1 or P-glycoprotein, for which experimental structures are known. (**a**) Schematic of the ABCB5 protein topology with the conserved domains indicated as blocks, including transmembrane domains (TMD) and nucleotide binding domains (NBD). Somatic alterations are represented by arrowheads. A total of 71 different alterations were identified, and for clarity, only some amino acid changes were indicated. Underlined alterations were functionally assessed. Red triangles represent deleterious alterations, blue triangles represent missense mutations, the orange triangle represents splice site, and purple triangles represent silent mutations. (**b**) Ribbon diagram of the full-length ABCB5 model, with the N-terminal transmembrane domain, or TMD1 in red and the C-terminal TMD2 in cyan. The N-terminal NBD1 and the C-terminal NBD2 are shown in yellow and green, respectively. Residues where mutations were found are displayed as ball models. (**c**) Residues S830 in the TM8 is shown in magenta, and residues S1091 and S1184 in NBD2 are colored in orange. (**d**) Magnified view of NBD2 showing detailed structural environment in the vicinity of the two mutation sites in ball models in orange. The Walker A and B motifs are colored light orange and pink, respectively. The signature motif is in purple. The two intracellular helical motifs are shown in cyan and red, respectively.

CDKN2A. The 63T cell line carries WT ABCB5, WT BRAF, nonsense mutant PTEN R130*, and knockout mutant CDKN2A del. Ex 1, 2, 3. SK-Mel-28 and A375 human melanoma cell lines were also chosen to test the impact of the ABCB5 mutants in a mutated BRAF genetic background. Both cell lines carry WT ABCB5, WT NRAS, and mutated BRAF. Furthermore, SK-Mel-28 cells carry WT CDKN2A, while A375 cells carry a partial deletion of CDKN2A (Poliseno et al., 2011).

Clones of human melanoma cell lines 17T and 63T were produced that stably overexpressed either WT ABCB5 or mutants of ABCB5 (Q187*, S830F, S1091F, S1184P). To investigate the possible effects of ABCB5 on melanoma cell growth, in vitro proliferation on plastic was first examined. All 17T clones overexpressing ABCB5 mutants have a statistically highly significant increased proliferation rate compared with the WT ABCB5 clone (Figure 3a). The impact of the ABCB5 mutations is lower in the 63T cells except for S1184P, for which the increase of the proliferation rate is highly statistically significant compared with the parental WT 63T cells (Figure 3b).

The proliferation rates of A375 WT ABCB5 and mutant clones were identical to parental cells (see Supplementary Figure S1a online). SK-Mel-28 clones overexpressing either the Q187* or S1184P mutations had significantly increased proliferation rates compared with parental cells and the other clones (see Supplementary Figure S1b). Additionally, the Q187* and S1184P clones displayed a reduced adhesion capacity and did not fully attach to plastic until 48 hours after seeding. Stable knockdown of ABCB5 in A375 cells had no effect on cell proliferation (see Supplementary Figure S1c). In contrast, stable knockdown of ABCB5 in SK-Mel-28 cells resulted in a significantly increased proliferation rate (see Supplementary Figure S1d).

A proliferation assay indicates a difference in terms of the proliferation capacity of the cells, but it has the disadvantage in that the proliferation of the cells is influenced by their ability to adhere to plastic. Anchorage-independent growth, which is considered a hallmark of carcinogenesis, was next assayed with a standard soft agar assay (Figure 4). For both cell lines, colony number was significantly higher for cells expressing ABCB5 mutants compared with the WT ABCB5-

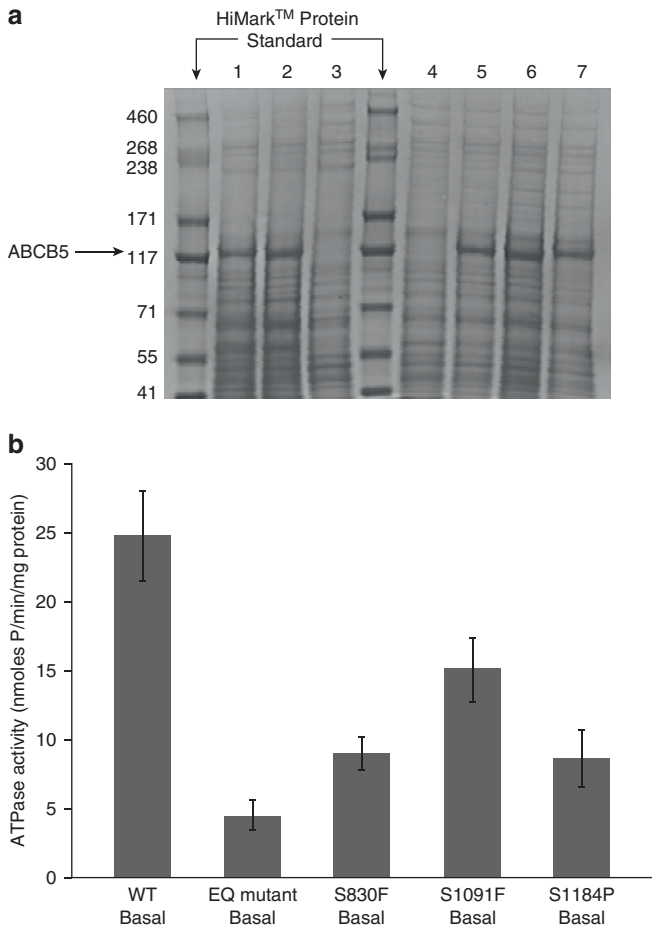

Figure 2. ATPase activity of ABCB5 WT and mutants. (**a**) ABCB5 WT and mutants were expressed in High Five insect cells, and 30 μg isolated crude membrane proteins were run in a Nupage Tris-acetate gel, along with a HiMark protein standard. All mutants were expressed in High Five insect cells to the same level as WT protein. (1) ABCB5 WT. (2) ABCB5 E1181Q mutant (nonfunctional transporter, negative control). (3) Crude membranes (negative control). (4) ABCB5-FLAG Q187*. (5) ABCB5-FLAG S830F. (6) ABCB5-FLAG S1091F. (7) ABCB5-FLAG S1184P. (**b**) ATPase activity of ABCB5 WT and ABCB5 mutants (E1181Q, S830F, S1091F, and S1184P) in High Five cell crude membranes was measured by endpoint Pi assay. WT and mutant ABCB5-specific ATPase activities were recorded as beryllium fluoride-sensitive ATPase activity. (Error bars denote standard deviation; n= 3). For the same expression level, we observed a decrease in the ATPase activity for the cells overexpressing ABCB5 mutants compared with the cells overexpressing ABCB5 WT. EQ, E1181Q; WT, wild type.

expressing cells. Again for this assay, we observed a greater effect for the 17T cell line ($P < 0.0001$ for each mutation except for the mutation S1091F, for which $P < 0.001$) (Figure 4a) than for the 63T cell line ($P < 0.0001$ for S830F and S1091F, $P < 0.05$ for the mutations Q187* and S1184P) (Figure 4b).

In both the SK-Mel-28 and A375 cell lines examined, colony numbers were not different, but colony sizes varied. In the A375 cell line, all four ABCB5 mutant clones formed significantly larger colonies compared with parental cells (see Supplementary Figure S2a online). When we examined SK-Mel-28 cells, only the Q187* and S1184P mutant clones had significantly larger colonies compared with parental cells (see Supplementary Figure S2b). In addition to overexpression of various ABCB5 clones, A375 and SK-Mel-28 clonal cell lines were produced that stably expressed either a nontargeting short hairpin RNA (shRNA) or an ABCB5-specific shRNA (see Supplementary Figure S2c). In both cell lines, stable knockdown of ABCB5 resulted in significantly larger colonies in soft agar, corroborating the overexpression data (see Supplementary Figure S2d).

Overall, we observed that the impact of the ABCB5 mutant expression on the proliferation capacities of melanoma cells is greater in cell lines that carry the activated mutant NRAS Q61K compared with those carrying the activated mutant BRAF. Furthermore, the impact of ABCB5 mutant expression was greater in 17T cells compared with 63T. This can be explained by the expression of heterozygous nonsense mutant ABCB5 Q187* in 17 cells, whereas 63T cells carry a homozygous WT ABCB5.

Impact of the mutations on development of metastases

A possible role of ABCB5 mutants in melanoma cell migration and invasion was then examined. For this, cells were seeded in a Boyden chamber in serum-free medium and were allowed to migrate through the pores to the other side of the semipermeable membrane in a serum-enriched medium compartment. In the invasion assay, cells must be able to digest the three-dimensional Matrigel (Corning Inc, Corning, NY) layer located at the bottom of the Boyden chamber. The cells were stained and counted after a 24-hour period. The 17T ABCB5 clones showed a higher migration ability for the mutations Q187* and S1091F, whereas the cells overexpressing ABCB5 S830F were not able to migrate through the pores of the Boyden chamber membrane (Figure 5a). The migration ability of 63T mutant ABCB5 clones was also affected and was significant for the mutations S830F and S1091F (Figure 5b). Both 17T (Figure 5c) and 63T cells (Figure 5d) were not able to invade through the Matrigel layer, except for the 63T S830F mutant.

In both A375 (see Supplementary Figure S3a online) and SK-Mel-28 (see Supplementary Figure S3b) cell lines, there was a slight trend toward increased invasion of the ABCB5 mutant clones, along with a trend toward reduced invasion in WT ABCB5 clones. For both the A375 and SK-Mel-28 cell lines, stable knockdown of ABCB5 resulted in a significant increase in invasive capacity (see Supplementary Figure S3c).

In summary, the combination of genetic, biochemical, and cellular data presented here suggests that loss of ABCB5 gene function accelerates the development of melanoma. Indeed, in experiments performed in four separate melanoma cell lines, either mutation of ABCB5 or loss of ABCB5 expression resulted in increased proliferative capacities, which were higher in cells with a mutated NRAS genetic background compared with a mutated BRAF background. However, the invasive capacities of ABCB5 mutant clones was observed only in mutated BRAF cell lines. In an NRAS background, ABCB5 mutant clones were able to migrate only through the membrane pores. The ABCB5 mutations are presumed to reduce ABCB5 transporter activity in the melanoma lines, with the possibility that some mutations may have dominant negative effects. Overall, these data indicate that ABCB5 is a potential tumor suppressor in melanoma. The physiological role of ABCB5 remains to be unraveled. However, we can

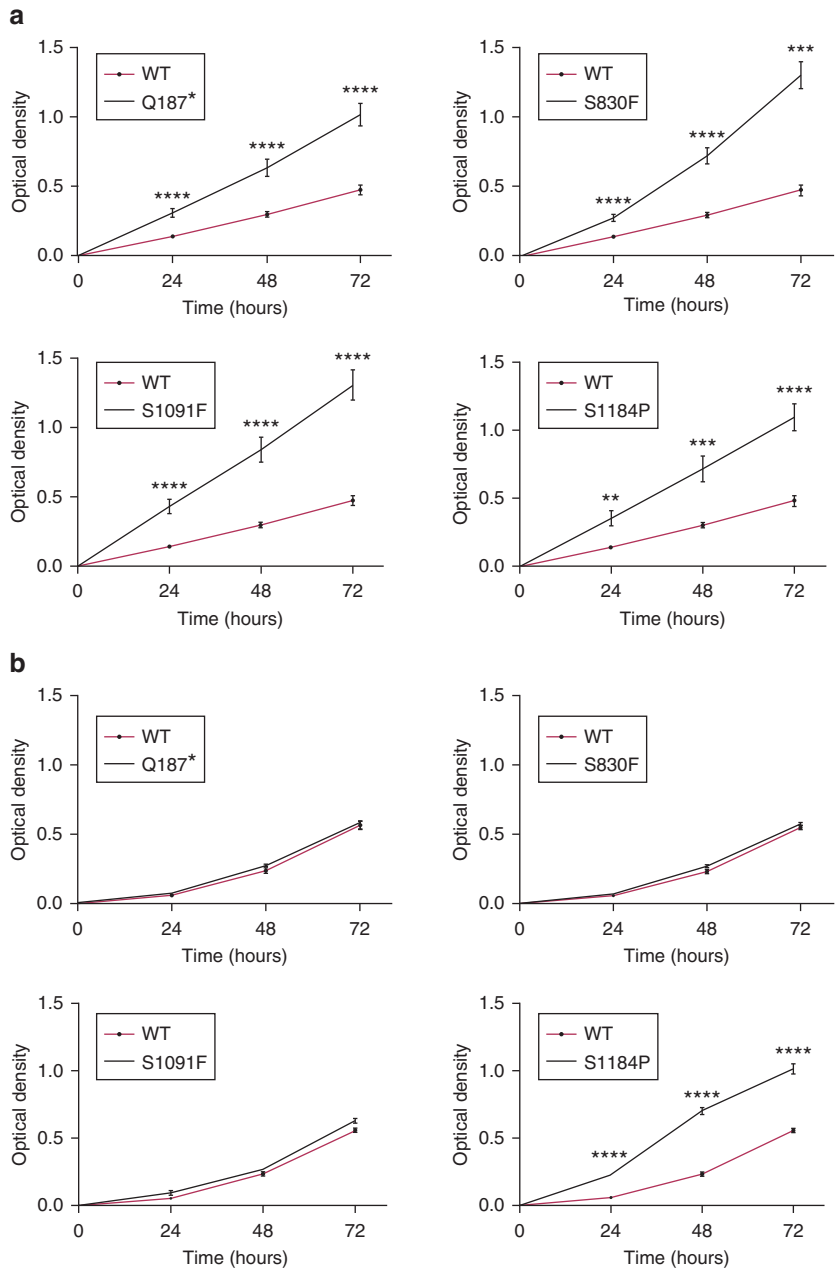

Figure 3. Effects of ABCB5 mutations on proliferation of melanoma cells. (**a**) Proliferation rates of 17T clones were assayed over 3 days. All 17T clones overexpressing ABCB5 mutants had a significant increase of their proliferation rate compared with the ABCB5 WT-overexpressing clone for each time point. (**b**) Proliferation rates of 63T ABCB5 clones were measured 3 and 4 days after seeding. The proliferation rate of the S1184P mutant was found to be very highly statistically significant only when compared with the parental WT 63T cells. $*P < 0.05$, $**P < 0.01$, $***P < 0.001$,$****P < 0.0001$. n = 4. Values are the mean ± standard error of the mean. WT, wild type.

speculate that once this transporter is no longer functional, there are physiological changes that affect cell metabolism and/or mutagenesis related to toxic reactive oxygen species (Kondo et al., 2015). BRAF inhibitors alone or in combination with MEK inhibitors exert immunomodulatory effects on the tumor and its microenvironment (Deken et al., 2016; Hu-Lieskovan et al., 2015). It would be interesting to assess combined BRAF-MEK inhibition in vitro, and also with PD-1 blockade in vivo, in mice recapitulating these genetic alterations.

MATERIALS AND METHODS

Tumor tissues

All human samples were obtained after written informed patient consent was given. Tissue and melanoma cell lines used for the Discovery and Prevalence Screen in this study were described previously (Palavalli et al., 2009). Tissues used for validation set 1 were fresh frozen melanoma tumors obtained from the National Cancer Institute Surgery Branch (see Supplementary Table S2 online). Tissue was collected at the NCI Medical Center, under institutional review board protocols. DNA was isolated from enriched macrodissected tumor isolates as previously described (see http://www.riedlab.nci.nih.gov). Tissue processing and storage were previously described by Morente et al. (2006). Tissues used for validation set 2 of melanomas were obtained from optimum cutting temperature-embedded frozen clinical specimens from the Melanoma Informatics, Tissue Resource, and Pathology Core (MelCore) at The University of Texas MD Anderson Cancer Center under institutional review board-approved protocols. DNA isolation from the tumor-enriched isolates has been described previously (Davies et al., 2009). Tissue was further collected, and cell lines were established at Queensland Institute of Medical Research (41 stage III and 46

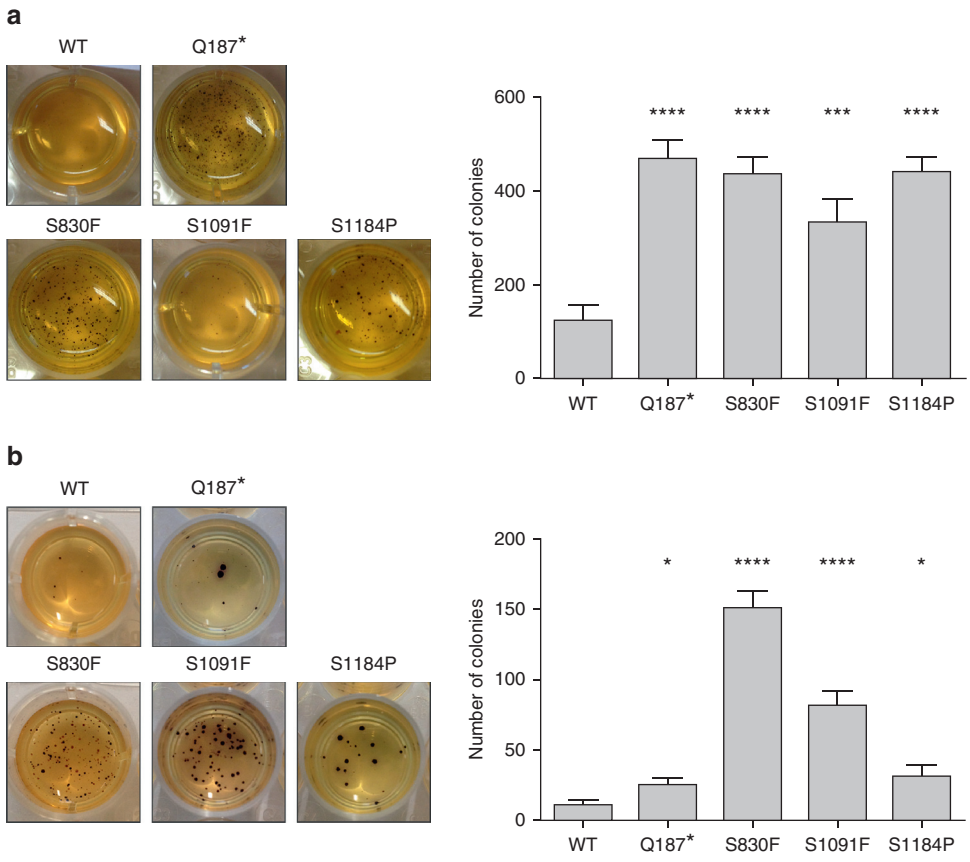

Figure 4. Effects of ABCB5 mutations on anchorage-independent growth of melanoma cells. (**a**) All 17T ABCB5 mutant clones had a highly significant increase in number of colonies compared with the 17T ABCB5 WT clone. (**b**) The 63T mutant clones showed a highly significant increase in number of colonies only for the mutations S830F and S1091F, whereas the effect was lower for the Q187* and S1184P mutations. $*P < 0.05$, $**P < 0.01$, $***P < 0.001$, $****P < 0.0001$. n = 3. Values are the mean ± standard error of the mean. WT, wild type.

stage IV (American Joint Committee on Cancer) early-passage metastatic melanoma cell lines). All cell lines were established as described previously (Castellano et al., 1997; Dutton-Regester et al., 2012; Pavey et al., 2004) with written informed patient consent under a protocol approved by the Queensland Institute of Medical Research Human Research Ethics Committee.

DNA extraction

DNA was extracted with a DNeasy Blood and Tissue kit (Qiagen, Hilden, Germany), following the manufacturer's instructions. DNA was eluted in 35 µl of elution buffer. DNA measurements were made with a ND-1000 UV-Vis spectrophotometer from NanoDrop Technologies (Wilmington, DE).

Whole-exome and genome sequencing

Whole-exome and genome sequencing was described previously (Gartner et al., 2013), and results have been deposited in the dbSNP, ClinVar database with the batch identification 1057273.

Sanger sequencing

PCR and sequencing primers were designed with Primer 3 (http://www-genome.wi.mit.edu/cgibin/primer/primer3_www.cgi) and synthesized by Integrated DNA Technologies (Coralville, IA) (see Supplementary Table S3 online). PCR amplification was performed as previously described (Samuels et al., 2004), and PCR products were purified with exonuclease (Epicentre Biotechnologies, Madison, WI) and shrimp alkaline phosphatase (USB Corporation, Cleveland, OH). Products were purified with rehydrated Sephadex G-50 powder (GE Healthcare, Piscataway, NJ), and cycle sequencing was carried out with a BigDye Terminator v3.1 Cycle Sequencing kit (Applied Biosystems, Foster City, CA). Sequence data were collected on an ABI3730xl (Applied Biosystems). Sequence traces of the secondary screen were analyzed with the Mutation Surveyor software package (SoftGenetics, State College, PA).

ATPase assay

ATPase activity of ABCB5 WT and mutated ABCB5 (E1181Q, S830F, S1091F, and S1184P) in High Five cell crude membranes was measured by an endpoint inorganic phosphate assay as described by Ambudkar (1998). The E1181Q mutation is found in the second nucleotide binding domain and renders the ABCB5 transporter nonfunctional. This mutant was produced as a negative control. A FLAG-tag was inserted in the first extracellular loop. ABCB5- and mutated ABCB5-specific ATPase activities were recorded as beryllium fluoride-sensitive ATPase activity as described by Ambudkar (1998).

Cell culture

The human melanoma cell lines 17T and 63T were cultured in RPMI media supplemented with 10% fetal clone serum, 1% penicillin/streptomycin, 1% L-Glut and HEPES (Life Technologies, Carlsbad, CA). The human melanoma cell lines A375 and SK-Mel-28 were cultured in RPMI media supplemented with 10% fetal bovine serum and 1% penicillin/streptomycin. Cells were maintained at 37 °C in a humidified atmosphere of 5% CO_2.

Lentiviral ABCB5 WT and mutated ABCB5 production

Lentiviral ABCB5-FLAG tag plasmid DNAs (ABCB5-FLAG tag WT - M01, ABCB5-FLAG Q187* - M02, ABCB5-FLAG S830F - M03, ABCB5-FLAG S1091F - M04, and ABCB5-FLAG S1184P - M05) were supplied by the Protein Expression Laboratory Cloning and Optimization Group (Frederick National Laboratory for Cancer

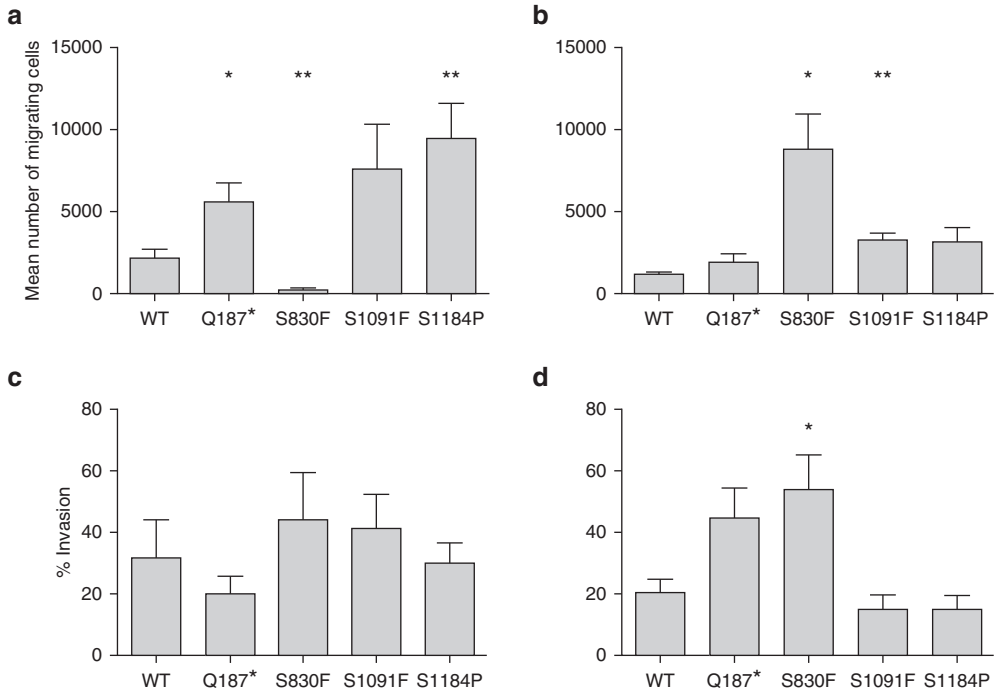

Figure 5. Effects of ABCB5 mutations on migratory and invasive abilities of melanoma cells. (**a**) 17T ABCB5 Q187*, S1091F, and S1184P mutant clones showed a higher migration ability, whereas the ABCB5 S830F mutant clone was not able to migrate from the upper side of the Boyden chamber to the lower one. (**b**) The migration ability of 63T ABCB5 mutant clones was also affected and was significant for the mutations S830F and S1091F. (**c**) The invasive ability of 17T ABCB5 WT and mutant clones was assessed, but no significant increase in invasion was observed. The *P* values (Student *t* test) are 0.4187 for Q187*, 0.5458 for S830F, 0.5856 for S1091F, and 0.8927 for the mutation S1184P. (**d**) The invasive ability of 63T ABCB5 WT and mutant clones was assessed, but no significant increase in invasion was observed, except for the S830F mutation. The *P* values (Student *t* test) are 0.0885 for Q187*, 0.0458 for S830F, 0.4291 for S1091F, and 0.4215 for S1184P. $*P < 0.05$, $**P < 0.01$, $***P < 0.001$, $****P < 0.0001$. n = 3. Values are the mean ± standard error of the mean.

Research, Frederick, MD). The HEK293T cells were cotransfected with the lentiviral envelope plasmid (pMD2.G, Addgene number 12259), the lentiviral packaging plasmid (psPAX2, Addgene number 12260), and one of the five lentiviral ABCB5-FLAG tag plasmid to generate lentivirus particles. The melanoma cell lines were infected with these lentivirus particles to overexpress either WT ABCB5 or one of the four ABCB5 mutats. Cells were selected by using 5 μg/ml puromycin. Sequencing was performed to assess the presence of WT or mutated ABCB5.

Proliferation assay

A total of 3,000 cells per well of A375 cells, 4,000 cells per well of SK-Mel-28 cells, or 4,500 cells per well of 17T and 63T cells were seeded into 96-well plates in complete RPMI media. At 24-hour time points (0, 24, 48, and 72 hours), growth media was removed and replaced with complete RPMI media solution containing a working concentration of 0.5 mg/ml 3-(4,5-dimethylthiazol-2-yl)-2,5-diphenyltetrazolium bromide (MTT) and incubated for 3 hours. Media with MTT was removed, and cells were solubilized in DMSO. Absorbance was measured at 570 nm on a SpectraMax i3 plate reader (Molecular Devices, San Jose, CA).

Soft agar colony formation assay

In each well of a 24-well plate, 4,500 cells (A375, SK-Mel-28) and 4,000 cells (17T, 63T) for all cell line clones were suspended in 0.33% Bacto-Agar (Sigma-Aldrich, St. Louis, MO), diluted in complete RPMI media. This layer was plated on top of a layer of 0.5% Bacto-Agar, diluted in complete RPMI media. Plates were maintained at 37 °C in a humidified atmosphere of 5% CO_2 for 3 weeks. Colonies were stained with 2 mg/ml MTT for 3 hours and then counted.

Transwell migration and Matrigel invasion assay

A total of 5×10^4 cells for A375 and SK-Mel-28 cell lines and clones and 12.5×10^3 cells for 17T and 63T cell lines were suspended in serum-free RPMI and pipetted into a Transwell insert (BD Biosciences, San Jose, CA) to assess their migration ability. The insert was placed into a well of a 24-well plate containing complete RPMI media and incubated for 24 hours at 37 °C in a humidified atmosphere of 5% CO_2. The same manipulation was performed for the invasion assay with a BioCat Matrigel Invasion chamber (Corning Inc). The inserts were washed with phosphate-buffered saline (to remove the nonmigrating and noninvading cells from the interior of the inserts) and stained with a Hema3 staining kit (Thermo Fisher Scientific, Waltham, MA). The migrating and invading cells were counted under a light microscope, and the percent invasion was calculated by the ratio between the mean number of invading cells and the mean number of migrating cells.

Statistical analysis

Data analysis was done by an unpaired Student *t* test or Welch *t* test when samples had unequal variances. Values are the means ± standard error of the mean. *P* values less than 0.05 were considered statistically significant. Statistics and graphing were done with Prism software (GraphPad, La Jolla, CA).

CONFLICT OF INTEREST

C-HL is an employee and shareholder of Natera. The other authors state no conflict of interest.

ACKOWLEDGMENTS

This work was supported by the Intramural Research Program of the National Institutes of Health, Center for Cancer Research, National Cancer Institute. YS is supported by the Israel Science Foundation (grant no. 696/17), the European Research Council under the European Union's Horizon 2020 research and innovation programme (grant agreement no. 770854), and the Minerva Foundation Grant. The authors acknowledge receiving the melanoma cells

from the Biospecimen Core of the Yale SPORE in Skin Cancer, funded by the National Cancer Institute, US National Institutes of Health, under award number 1 P50 CA121974. The authors also thank George Leiman for editorial assistance, Robert Rutledge (LCB, National Cancer Institute, National Institutes of Health, Bethesda, MD) and Michel Jadot (Molecular Physiology Research Unit, NAmur Research Institute for LIfe Sciences, University of Namur, Belgium) for critical comments and discussion. Finally, the authors are grateful to Laurent Duvivier and Florence Gaudray for their technical support on the migration/invasion assay.

SUPPLEMENTARY MATERIALS

Supplementary material is linked to the online version of the paper at www.jidonline.org, and at https://doi.org/10.1016/j.jid.2019.01.036.

REFERENCES

Ambudkar SV. Drug-stimulatable ATPase activity in crude membranes of human *MDR1*-transfected mammalian cells. Methods Enzymol 1998;292:504–14.

Berger MF, Hodis E, Heffernan TP, Deribe YL, Lawrence MS, Protopopov A, et al. Melanoma genome sequencing reveals frequent *PREX2* mutations. Nature 2012;485(7399):502–6.

Castellano M, Pollock PM, Walters MK, Sparrow LE, Down LM, Gabrielli BG, et al. *CDKN2A*/p16 is inactivated in most melanoma cell lines. Cancer Res 1997;57:4868–75.

Chartrain M, Riond J, Stennevin A, Vandenberghe I, Gomes B, Lamant L, et al. Melanoma chemotherapy leads to the selection of ABCB5-expressing cells. PLoS One 2012;7(5):e36762.

Chen KG, Szakács G, Annereau J-P, Rouzaud F, Liang X-J, Valencia JC, et al. Principal expression of two mRNA isoforms (*ABCB 5α* and *ABCB 5β*) of the ATP-binding cassette transporter gene *ABCB* 5 in melanoma cells and melanocytes. Pigment Cell Res 2005;18:102–12.

Davies MA, Stemke-Hale K, Lin E, Tellez C, Deng W, Gopal YN, et al. Integrated molecular and clinical analysis of AKT activation in metastatic melanoma. Clin Cancer Res 2009;15:7538–46.

Deken MA, Gadiot J, Jordanova ES, Lacroix R, van Gool M, Kroon P, et al. Targeting the MAPK and PI3K pathways in combination with PD1 blockade in melanoma. Oncoimmunology 2016;5(12):e1238557.

Dutton-Regester K, Aoude LG, Nancarrow DJ, Stark MS, O'Connor L, Lanagan C, et al. Identification of *TFG* (TRK-fused gene) as a putative metastatic melanoma tumor suppressor gene. Genes Chromosomes Cancer 2012;51:452–61.

Esser L, Zhou F, Pluchino KM, Shiloach J, Ma J, Tang WK, et al. Structures of the multidrug transporter P-glycoprotein reveal asymmetric ATP binding and the mechanism of polyspecificity. J Biol Chem 2017;292:446–61.

Fletcher JI, Williams RT, Henderson MJ, Norris MD, Haber M. ABC transporters as mediators of drug resistance and contributors to cancer cell biology. Drug Resist Updat 2016;26:1–9.

Frank NY, Margaryan A, Huang Y, Schatton T, Waaga-Gasser AM, Gasser M, et al. ABCB5-mediated doxorubicin transport and chemoresistance in human malignant melanoma. Cancer Res 2005;65:4320–33.

Frank NY, Pendse SS, Lapchak PH, Margaryan A, Shlain D, Doeing C, et al. Regulation of progenitor cell fusion by ABCB5 P-glycoprotein, a novel human ATP-binding cassette transporter. J Biol Chem 2003;278:47156–65.

Gartner JJ, Parker SC, Prickett TD, Dutton-Regester K, Stitzel ML, Lin JC, et al. Whole-genome sequencing identifies a recurrent functional synonymous mutation in melanoma. Proc Natl Acad Sci USA 2013;110:13481–6.

Gillet JP, Wang J, Calcagno AM, Green LJ, Varma S, Bunkholt Elstrand M, et al. Clinical relevance of multidrug resistance gene expression in ovarian serous carcinoma effusions. Mol Pharm 2011;8:2080–8.

Hodis E, Watson IR, Kryukov GV, Arold ST, Imielinski M, Theurillat JP, et al. A landscape of driver mutations in melanoma. Cell 2012;150:251–63.

Hu-Lieskovan S, Mok S, Homet Moreno B, Tsoi J, Robert L, Goedert L, et al. Improved antitumor activity of immunotherapy with BRAF and MEK inhibitors in *BRAF*^{V600E} melanoma. Sci Transl Med 2015;7(279):279ra41.

Kawanobe T, Kogure S, Nakamura S, Sato M, Katayama K, Mitsuhashi J, et al. Expression of human ABCB5 confers resistance to taxanes and anthracyclines. Biochem Biophys Res Commun 2012;418:736–41.

Keniya MV, Holmes AR, Niimi M, Lamping E, Gillet JP, Gottesman MM, et al. Drug resistance is conferred on the model yeast *Saccharomyces cerevisiae* by expression of full-length melanoma-associated human ATP-binding cassette transporter ABCB5. Mol Pharm 2014;11:3452–62.

Kondo S, Hongama K, Hanaya K, Yoshida R, Kawanobe T, Katayama K, et al. Upregulation of cellular glutathione levels in human *ABCB5*- and murine *Abcb5*-transfected cells. BMC Pharmacol Toxicol 2015;16:37.

Krauthammer M, Kong Y, Bacchiocchi A, Evans P, Pornputtapong N, Wu C, et al. Exome sequencing identifies recurrent mutations in *NF1* and RASopathy genes in sun-exposed melanomas. Nat Genet 2015;47:996–1002.

Li J, Jaimes KF, Aller SG. Refined structures of mouse P-glycoprotein. Protein Sci 2014;23:34–46.

Morente MM, Mager R, Alonso S, Pezzella F, Spatz A, Knox K, et al. TuBaFrost 2: standardising tissue collection and quality control procedures for a European virtual frozen tissue bank network. Eur J Cancer 2006;42:2684–91.

Nikolaev SI, Rimoldi D, Iseli C, Valsesia A, Robyr D, Gehrig C, et al. Exome sequencing identifies recurrent somatic *MAP2K1* and *MAP2K2* mutations in melanoma. Nat Genet 2011;44:133–9.

Palavalli LH, Prickett TD, Wunderlich JR, Wei X, Burrell AS, Porter-Gill P, et al. Analysis of the matrix metalloproteinase family reveals that *MMP8* is often mutated in melanoma. Nat Genet 2009;41:518–20.

Pavey S, Johansson P, Packer L, Taylor J, Stark M, Pollock PM, et al. Microarray expression profiling in melanoma reveals a *BRAF* mutation signature. Oncogene 2004;23:4060–7.

Poliseno L, Haimovic A, Christos PJ, Vega y Saenz de Miera EC, Shapiro R, Pavlick A, et al. Deletion of *PTENP1* pseudogene in human melanoma. J Invest Dermatol 2011;131:2497–500.

Samuels Y, Wang Z, Bardelli A, Silliman N, Ptak J, Szabo S, et al. High frequency of mutations of the *PIK3CA* gene in human cancers. Science 2004;304(5670):554.

Schatton T, Murphy GF, Frank NY, Yamaura K, Waaga-Gasser AM, Gasser M, et al. Identification of cells initiating human melanomas. Nature 2008;451(7176):345–9.

Sjoblom T, Jones S, Wood LD, Parsons DW, Lin J, Barber TD, et al. The consensus coding sequences of human breast and colorectal cancers. Science 2006;314(5797):268–74.

Stark MS, Woods SL, Gartside MG, Bonazzi VF, Dutton-Regester K, Aoude LG, et al. Frequent somatic mutations in *MAP3K5* and *MAP3K9* in metastatic melanoma identified by exome sequencing. Nat Genet 2011;44:165–9.

Wei X, Walia V, Lin JC, Teer JK, Prickett TD, Gartner J, et al. Exome sequencing identifies GRIN2A as frequently mutated in melanoma. Nat Genet 2011;43:442–6.

SUPPLEMENTARY MATERIALS AND METHODS

Lentiviral shRNA production and knockdown validation

pGIPZ shRNA constructs for stable knockdown of human ABCB5 were obtained from Open Biosystems (Huntsville, AL) (clone identification: V2LHS_100516, catalog no. RHS4430-200216400). A nonsilencing pGIPZ shRNA (catalog no. RHS4346) was used as a control. Lentiviral particles were made via Lipofectamine 2000 (Invitrogen, Waltham, MA)-mediated triple transfection of 293T cells with pGIPZ shRNA plasmids, along with the lentiviral envelope plasmid (pMD2.G, Addgene number 12259) and the lentiviral packaging plasmid (psPAX2, Addgene number 12260). Melanoma cells were transduced with either nonsilencing or ABCB5-specific shRNA containing lentiviral particles in the presence of 8 μg/ml polybrene, and stable cells were selected with 3 μg/ml puromycin for 1 week and were pooled before determining knockdown efficiency. Knockdown efficiency was determined with semiquantitative reverse transcriptase PCR. Total RNA was collected, following the manufacturer's protocol for the RNeasy Mini Kit (Qiagen). cDNA was synthesized with the iScript cDNA Synthesis Kit (Bio-Rad, Hercules, CA), by using 1 μg of total RNA. To test for knockdown of the ABCB5 message, 2 μl of cDNA with a human ABCB5-specific primer pair (QuantiTect Primer Assay, QT02394679; Qiagen) and a human β-actin–specific primer set were amplified in a PCR reaction with iQ SYBR Green Supermix (Bio-Rad) at a final volume of 50 μl. The PCR reaction program consisted of an initial 3 minutes at 95 °C and 40 cycles of 95 °C for 10 seconds and 55 °C for 45 seconds. PCR reaction results were visualized via agarose gel. ABCB5 pGIPZ shRNA (catalog no. RHS4430-99297707; Dharmacon, Lafayette, CO) gave the best knockdown in both cell lines and was used in functional studies.

SUPPLEMENTARY REFERENCES

Berger MF, Hodis E, Heffernan TP, Deribe YL, Lawrence MS, Protopopov A, et al. Melanoma genome sequencing reveals frequent *PREX2* mutations. Nature 2012;485(7399):502–6.

Hodis E, Watson IR, Kryukov GV, Arold ST, Imielinski M, Theurillat JP, et al. A landscape of driver mutations in melanoma. Cell 2012;150:251–63.

Krauthammer M, Kong Y, Ha BH, Evans P, Bacchiocchi A, McCusker JP, et al. Exome sequencing identifies recurrent somatic *RAC1* mutations in melanoma. Nat Genet 2012;44:1006–14.

Nikolaev SI, Rimoldi D, Iseli C, Valsesia A, Robyr D, Gehrig C, et al. Exome sequencing identifies recurrent somatic *MAP2K1* and *MAP2K2* mutations in melanoma. Nat Genet 2011;44:133–9.

Stark MS, Woods SL, Gartside MG, Bonazzi VF, Dutton-Regester K, Aoude LG, et al. Frequent somatic mutations in *MAP3K5* and *MAP3K9* in metastatic melanoma identified by exome sequencing. Nat Genet 2011;44:165–9.

Wei X, Walia V, Lin JC, Teer JK, Prickett TD, Gartner J, et al. Exome sequencing identifies GRIN2A as frequently mutated in melanoma. Nat Genet 2011;43:442–6.

Supplementary Figure S1. Effects of ABCB5 alterations on melanoma cell proliferation. **(a)** Proliferation rates of A375 parental cells and ABCB5 clones were assayed over 3 days. No differences in growth were noted. n = 2. **(b)** Proliferation rates of SK-Mel-28 parental cells and ABCB5 clones were measured 3 and 4 days after seeding. Clones overexpressing ABCB5 mutants, Q187* or S1184P, had increased growth rates. $P < 0.05$. n = 2. **(c)** Proliferation rates of control shRNA and ABCB5-specific shRNA A375 clones were measured over 3 days. No differences in growth were noted when ABCB5 was stably knocked down. n = 3. **(d)** Proliferation rates of control shRNA and ABCB5-specific shRNA SK-Mel-28 clones were measured over 3 days. Stable knockdown of ABCB5 increased growth at 48 and 96 hours. *$P < 0.05$. n = 3. Values are the means ± standard error of the mean. shRNA, short hairpin RNA.

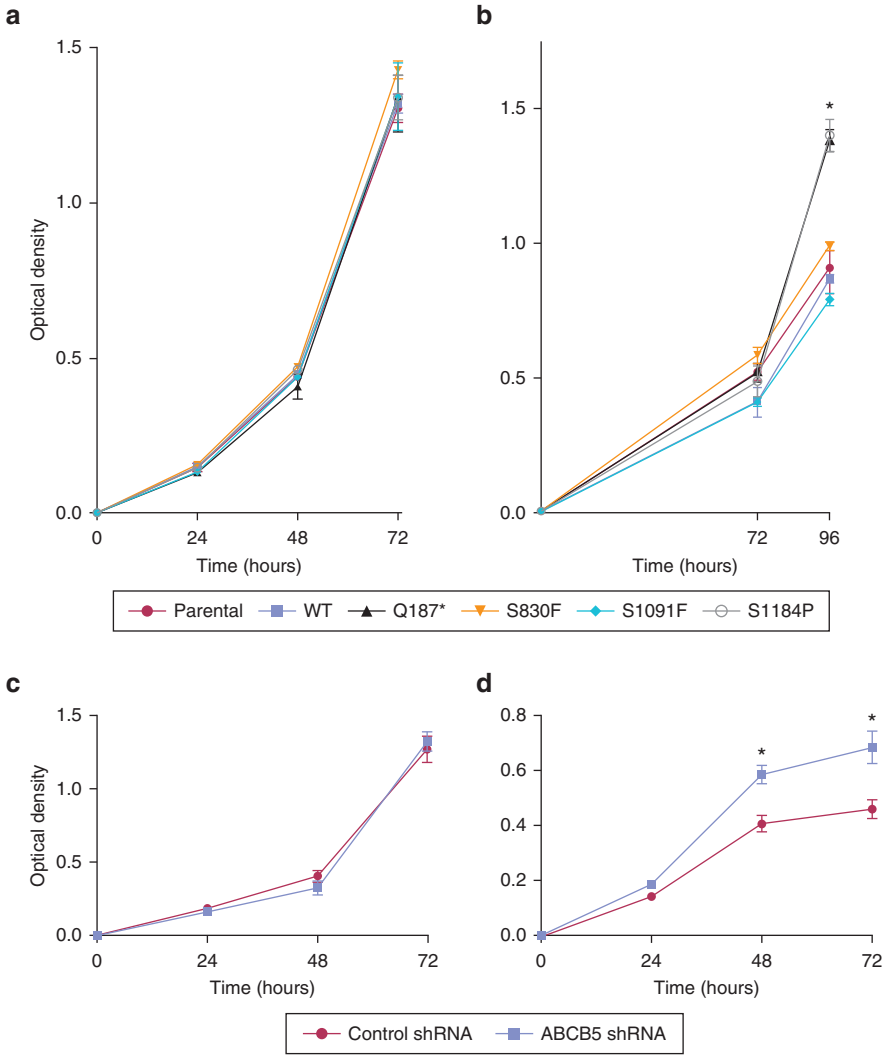

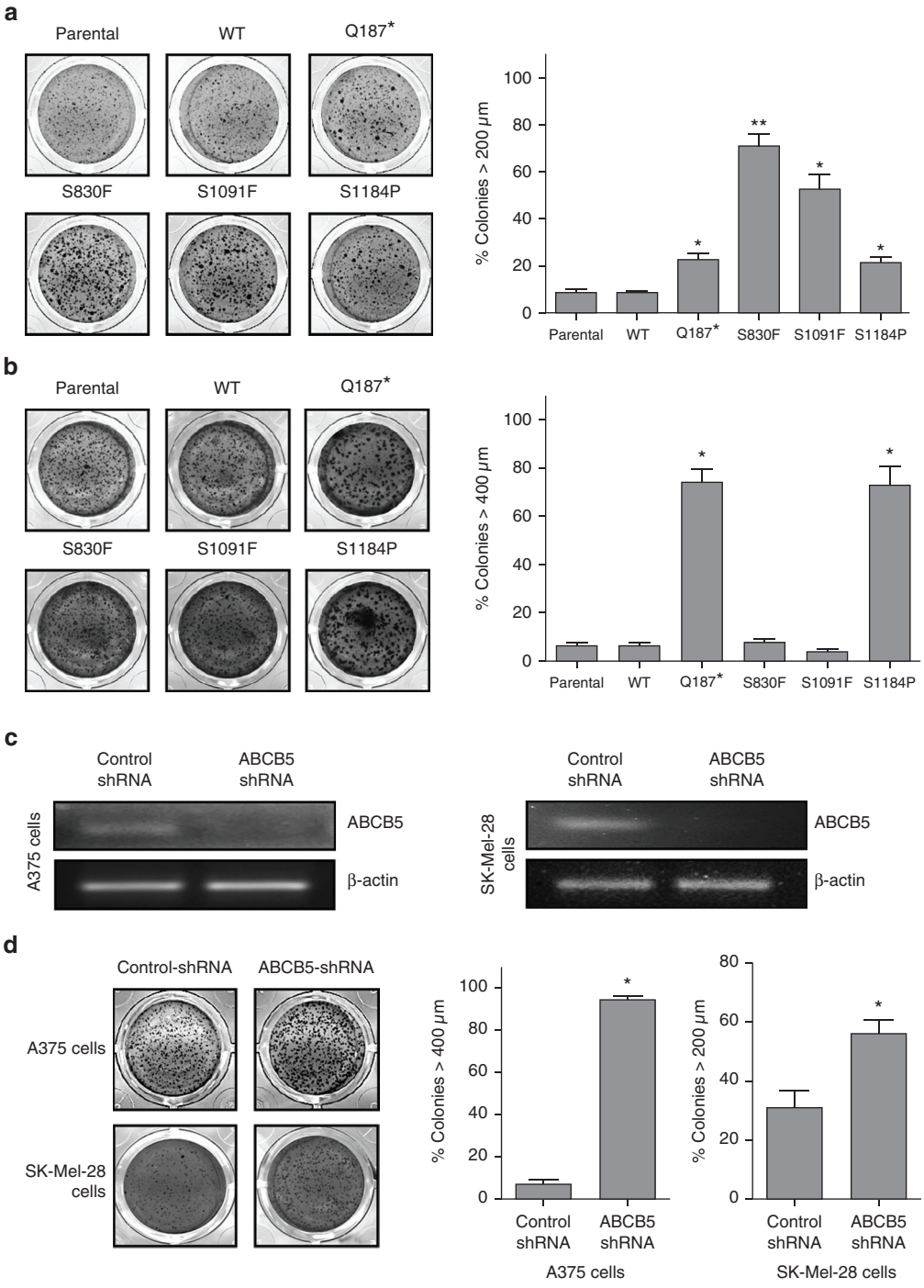

Supplementary Figure S2. Effects of ABCB5 alterations on anchorage-independent growth of melanoma cells. **(a)** All A375 ABCB5 mutant clones had a significant increase in percentage of colonies larger than 200 μm when grown in soft agar. $*P < 0.01$, $**P < 0.001$. n = 3. **(b)** SK-Mel-28 ABCB mutant clones Q187* and S1184P had a significant increase in the percentage of colonies larger than 400 μm when grown in soft agar. $*P < 0.001$. n = 3. **(c)** Stable expression of an ABCB5-specific shRNA resulted in near depletion of ABCB5 mRNA, as judged by reverse transcriptase PCR analysis. Stable expression of a nonsilencing shRNA was used as a control. **(d)** Stable knockdown of ABCB5 in both A375 and SK-Mel-28 cells resulted in a significant increase in the percentage of colonies larger than 400 and 200 μm, respectively, compared with control shRNA cells. $P < 0.0001$ for A375 cells and $P < 0.05$ for SK-Mel-28 cells. Representative images of wells are shown. Values are mean ± standard error of the mean. In each case, 200 colonies were counted. shRNA, short hairpin RNA; WT, wild type.

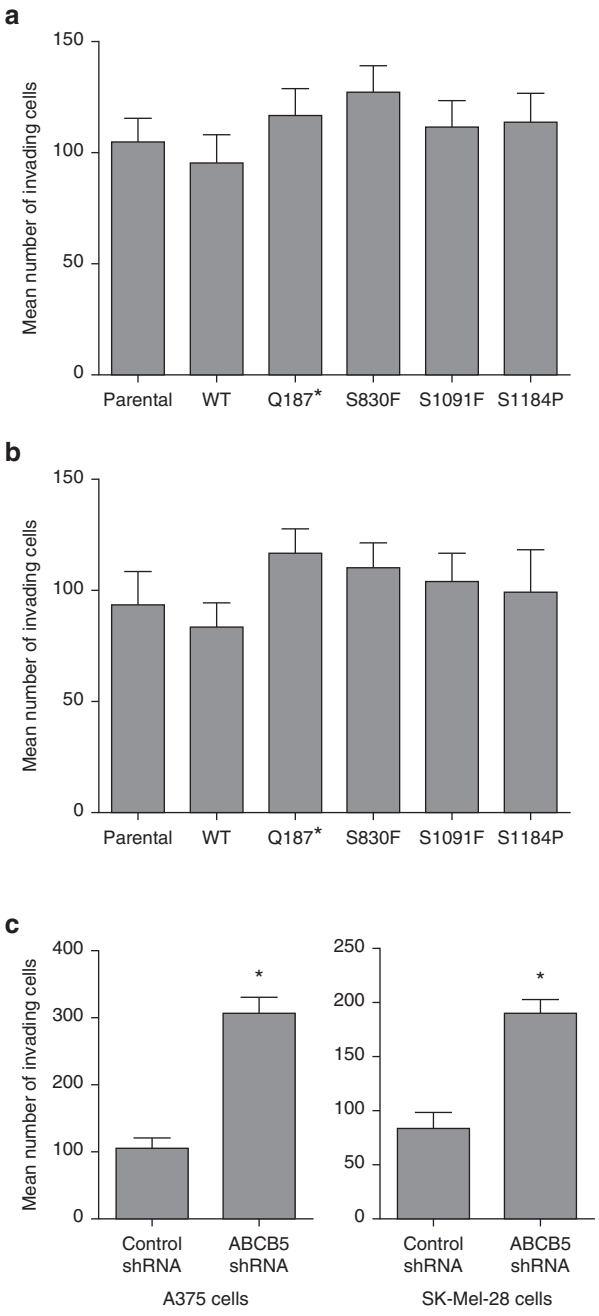

Supplementary Figure S3. Effects of ABCB5 alterations on the invasive abilities of melanoma cells. **(a)** A375 parental cells and ABCB5 clones were placed in invasion wells, and the ability to invade through a Matrigel matrix over 24 hours was examined. No significant changes in invasive abilities between various ABCB5 clones and parental cells were noted. **(b)** Similarly, no significant changes in invasive abilities were noted in SK-Mel-28 cells. **(c)** For both A375 and SK-Mel-28 cells, stable knockdown of ABCB5 caused a significant increase in invasion through Matrigel compared with control shRNA cells. $*P < 0.01$. For all invasion assays, $n = 3$. Values are mean ± standard error of the mean. shRNA, short hairpin RNA; WT, wild type.

Supplementary Table S1. ABCB5 Mutations in 487 Samples[1]

Gene	Sample	Mutation	Mutation Type
NM_001163941.1	12T	I828I	Silent
	17T	Q187*	Nonsense
	2427TIL	S979F	Missense
	24T	S1091F	Missense
	2556TIL	V827I	Missense
	2556TIL	S830F	Missense
	32T	S1184P	Missense
	55T	E520D	Missense
	55T	Q1098*	Nonsense
	D35	G598E	Missense
	LAU165	E1083fs	Frame_Shift_Ins
	LAU50_1&2	F739F	Silent
	ME012	F751F	Silent
	ME044	G485R	Missense
	MEL-JWCI-14-Tumor	D44N	Missense
	MEL-JWCI-14-Tumor	D780N	Missense
	MEL-JWCI-WGS-11-Tumor	F1022S	Missense
	MEL-JWCI-WGS-12-Tumor	A497T	Missense
	MEL-JWCI-WGS-18-Tumor	Q779*	Nonsense
	MEL-JWCI-WGS-1-Tumor	G1055G	Silent
	MEL-JWCI-WGS-22-Tumor	D780N	Missense
	MEL-JWCI-WGS-8-Tumor	V1210V	Silent
	MEL-Ma-Mel-08a-Tumor	I507I	Silent
	MEL-Ma-Mel-119-Tumor	F1023F	Silent
	MEL-Ma-Mel-65-Tumor	S830F	Missense
	MEL-Ma-Mel-67-Tumor	N883K	Missense
	MEL-Ma-Mel-94-Tumor	P647L	Missense
	MEL-UKRV-Mel-24-Tumor	Q779*	Nonsense
	TCGA-BF-A3DL-01A-11D-A20D-08	S983L	Missense
	TCGA-D3-A3MR-06A-11D-A21A-08	S638L	Missense
	TCGA-D9-A148-06A-11D-A19A-08	S638L	Missense
	TCGA-D9-A149-06A-11D-A196-08	R587Q	Missense
	TCGA-D9-A1JX-06A-11D-A19A-08	I577I	Silent
	TCGA-DA-A1HY-06A-11D-A19A-08	F751F	Silent
	TCGA-DA-A1I5-06A-11D-A197-08	H926Y	Missense
	TCGA-DA-A1I7-06A-22D-A197-08	R1027C	Missense
	TCGA-EB-A24D-01A-11D-A197-08	G179R	Missense
	TCGA-EE-A180-06A-11D-A21A-08	G721E	Missense
	TCGA-EE-A181-06A-11D-A196-08	R587Q	Missense
	TCGA-EE-A181-06A-11D-A196-08	G758C	Missense
	TCGA-EE-A182-06A-11D-A196-08	N1133I	Missense
	TCGA-EE-A20B-06A-11D-A196-08	S645S	Silent
	TCGA-EE-A20H-06A-11D-A197-08	K980I	Missense
	TCGA-EE-A29D-06A-11D-A197-08	E520K	Missense
	TCGA-EE-A29D-06A-11D-A197-08	G754E	Missense
	TCGA-EE-A29D-06A-11D-A197-08	G814S	Missense
	TCGA-EE-A29D-06A-11D-A197-08	F896F	Silent
	TCGA-EE-A29D-06A-11D-A197-08	D1187N	Missense
	TCGA-EE-A29E-06A-11D-A197-08	D624_splice	Splice_Site
	TCGA-EE-A29M-06A-11D-A196-08	P674S	Missense
	TCGA-EE-A29M-06A-11D-A196-08	I805F	Missense
	TCGA-EE-A29W-06A-11D-A196-08	G1229E	Missense
	TCGA-EE-A2GC-06A-11D-A197-08	R587*	Nonsense
	TCGA-EE-A2GC-06A-11D-A197-08	G1055G	Silent
	TCGA-EE-A2GI-06A-11D-A196-08	A895A	Silent
	TCGA-EE-A2GL-06A-11D-A196-08	R587Q	Missense
	TCGA-EE-A2GO-06A-11D-A196-08	R1027C	Missense
	TCGA-EE-A2MI-06A-11D-A197-08	G1005G	Silent

(*continued*)

Supplementary Table S1. Continued

Gene	Sample	Mutation	Mutation Type
	TCGA-EE-A2MJ-06A-11D-A197-08	S710F	Missense
	TCGA-EE-A2MR-06A-11D-A196-08	R613Q	Missense
	TCGA-EE-A2MS-06A-11D-A197-08	G1005G	Silent
	TCGA-EE-A2MS-06A-11D-A197-08	R1168K	Missense
	TCGA-EE-A3AA-06A-11D-A196-08	P647S	Missense
	TCGA-EE-A3AE-06A-11D-A196-08	M949I	Missense
	TCGA-EE-A3AG-06A-31D-A196-08	M525I	Missense
	TCGA-EE-A3J5-06A-11D-A20D-08	E869E	Silent
	TCGA-FS-A1Z7-06A-11D-A197-08	R486Q	Missense
	TCGA-FS-A1ZB-06A-12D-A197-08	S638S	Silent
	TCGA-FS-A1ZK-06A-11D-A197-08	R138R	Silent
	TCGA-FS-A1ZK-06A-11D-A197-08	P1121L	Missense
	TCGA-FS-A1ZM-06A-12D-A197-08	E630K	Missense
	TCGA-FS-1ZZ-06A-11D-A197-08	D629N	Missense
	TCGA-GN-A265-06A-21D-A197-08	R938Q	Missense
	TCGA-GN-A266-06A-11D-A197-08	D597N	Missense
	TCGA-GN-A269-01A-11D-A19A-08	S830F	Missense
	TCGA-IH-A3EA-01A-11D-A20D-08	S811F	Missense
NM_001163941.1	YUAVEY	R587Q	Missense
	YUDAB	S830F	Missense
	YUDUTY	M737I	Missense
	YUGISMO	G947E	Missense
	YUGOE	R587*	Nonsense
	YUMER	S912L	Missense
	YUPROST	S650F	Missense
	YURTHE	F1137L	Missense
	YURUS	D597N	Missense

[1]Results from mutational data in published studies (Berger et al., 2012; Hodis et al., 2012; Krauthammer et al., 2012; Nikolaev et al., 2011; Stark et al., 2011; Wei et al., 2011) combined with The Cancer Genome Atlas exome data.

Supplementary Table S2. Clinical Sample Information

Sample	Patient Age in Years[1]	Patient Sex	Characteristic	Primary Tumor Site	Metastatic Tumor Site	Matched Normal Source
1T[2]	29	F	Cutaneous	Posterior neck	Lung	Blood
5T[2]	47	M	Cutaneous	Lower abdomen	Iliac	Blood
6T	42	M	Cutaneous	Temple	Neck, soft tissue	Blood
7T[2]	53	M	Cutaneous	Knee	Stomach	Blood
8T[2]	61	M	Cutaneous	Thigh	Inguinal	Blood
9T[2]	62	M	Cutaneous	Mid-back	Back, subcutaneous	Blood
12T[2]	53	M	Cutaneous	Arm	Upper arm, subcutaneous	Blood
14T[2]	58	F	Cutaneous	Foot	Small bowel	Blood
16T	62	M	Cutaneous	Scalp	Lung	Blood
17T[2]	33	M	Cutaneous	Unknown	Shoulder, subcutaneous	Blood
18T[2]	55	M	Cutaneous	Upper back	Clavicle, soft tissue	Blood
20T	58	F	Cutaneous	Shoulder	Axilla	Blood
22T[†]	51	M	Cutaneous	Nipple	Chest wall, subcutaneous	Blood
23T[2]	44	M	Cutaneous	Scalp	Lung	Blood
24T[2]	49	M	Cutaneous	Upper arm	Axilla	Blood
26T[2]	48	F	Cutaneous	Upper thigh	Lung	Blood
29T	51	M	Cutaneous	Thigh	Inguinal	Blood
32T[2]	58	M	Cutaneous	Shoulder	Omentum	Blood
35T[2]	23	F	Cutaneous[3]	Heel	Thigh, subcutaneous	Blood
43T[2]	19	F	Cutaneous	Thigh	Popliteal soft tissue	Blood
44T	56	M	Cutaneous	Mid-back	Lung	Blood
51T[2]	50	F	Cutaneous	Medial thigh	Adnexa	Blood
55T[2]	60	M	Cutaneous	Neck	Lung	Blood
56T[2]	52	M	Cutaneous	Thigh	Lung	Blood
60T[2]	46	M	Cutaneous	Abdomen	Flank, subcutaneous	Blood
64T[2]	32	F	Cutaneous	Unknown	Ovary	Blood
79T	53	M	Cutaneous	Mid-back	Supraclavicular, soft tissue	Blood
81T[2]	60	F	Cutaneous	Arm	Upper arm, subcutaneous	Blood
83T	33	F	Cutaneous	Arm	Back, subcutaneous	Blood
84T	60	F	Cutaneous	Calf	Thigh, subcutaneous	Blood
86T	42	F	Cutaneous	Forearm	Liver	Blood
88T[2]	37	F	Cutaneous	Scalp	Chest wall, subcutaneous	Blood
90T	19	M	Cutaneous	Occipital scalp	Neck, soft tissue	Blood
91T[2]	55	F	Cutaneous	Shoulder	Subcostal soft tissue	Blood
92T	37	F	Cutaneous	Inguinal	Femur	Blood
93T[2]	42	F	Cutaneous	Finger	Axilla	Blood
95T	58	F	Cutaneous	Unknown	Inguinal	Blood
96T[2]	49	M	Cutaneous	Unknown	Inguinal	Blood
105T	28	M	Cutaneous	Upper back	Neck, soft tissue	Blood
108T[2]	25	F	Cutaneous	Heel	Thigh, subcutaneous	Blood
109T	58	M	Cutaneous	Shoulder	Scrotum	Blood
110T	51	M	Cutaneous	Unknown	Axilla	Blood
111T	41	M	Cutaneous	Mid-upper back	Axilla	Blood
112T	46	M	Cutaneous	Lower back	Inguinal	Blood
113T	38	M	Cutaneous	Posterior shoulder	Axilla	Blood
114T	22	M	Cutaneous	Unknown	Adrenal gland	Blood
116T	29	M	Cutaneous	Leg	Thigh, subcutaneous	Blood
117T	44	M	Cutaneous	Posterior lower leg	Chest wall, subcutaneous	Blood
119T	45	M	Cutaneous	Chest	Axilla	Blood
122T	60	F	Cutaneous	Back	Lung	Blood
123T	51	M	Cutaneous	Unknown	Anticubital	Blood
124T	44	M	Cutaneous	Back	Inguinal	Blood
125T	27	M	Cutaneous	Upper back	Axilla	Blood
130T[2]	49	F	Cutaneous	Lower extremity	Thigh, subcutaneous	Blood

Abbreviations: F, female; L, left; LN, lymph node; M, male; R, right.
[1]Patient's age when tumor was surgically removed.
[2]Samples used in exome/genome sequencing.
[3]Acral lentiginous.

Supplementary Table S3. PCR primer sequences

Sequence Name	Sequence
Forward primers	
NM_001163941_cds_1_0_chr7_20629434_f.fwd	TGTAAAACGACGGCCAGTGATGCTTCCTTTTTCAAACTGTG
NM_001163941_cds_2_0_chr7_20632705_f.fwd	TGTAAAACGACGGCCAGTCAAGTTTACAGACAACCAGTGACAA
NM_001163941_cds_3_0_chr7_20634836_f_1.fwd	TGTAAAACGACGGCCAGTTGATTTTATGCACTTATTTACCATC
NM_001163941_cds_4_0_chr7_20638207_f.fwd	TGTAAAACGACGGCCAGTCTGCGTGTGGGCAGTAAAT
NM_001163941_cds_5_0_chr7_20649332_f_1.fwd	TGTAAAACGACGGCCAGTCACTCTATGTTTTACCAGGAAACCT
NM_001163941_cds_6_0_chr7_20649609_f_1.fwd	TGTAAAACGACGGCCAGTTGTTGCTGCCTTGATTTTTG
NM_001163941_cds_6_0_chr7_20649609_f_2.fwd	TGTAAAACGACGGCCAGTTCAGTGATGGTATTGGAGATAAGA
NM_001163941_cds_7_0_chr7_20651904_f_1.fwd	TGTAAAACGACGGCCAGTAGGTAAACCTGTCTAGTCACCAA
NM_001163941_cds_8_0_chr7_20652109_f_1.fwd	TGTAAAACGACGGCCAGTGGTCATCTCATTGACCAGTAAGG
NM_001163941_cds_8_0_chr7_20652109_f_2.fwd	TGTAAAACGACGGCCAGTTGTCTCTTGGTGCTGTGTACTTC
NM_001163941_cds_9_0_chr7_20653683_f_1.fwd	TGTAAAACGACGGCCAGTGGTCATATCTTCCATTCTTTCTTACC
NM_001163941_cds_10_0_chr7_20654116_f_1.fwd	TGTAAAACGACGGCCAGTAAGAGGAGATTGTGTTGTATTGAAA
NM_001163941_cds_11_0_chr7_20656170_f_1.fwd	TGTAAAACGACGGCCAGTTGTACATGAAACAAACATAACAAGA
NM_001163941_cds_12_0_chr7_20657568_f_1.fwd	TGTAAAACGACGGCCAGTGGTGCCCATCTACCAGAAAA
NM_001163941_cds_12_0_chr7_20657568_f_2.fwd	TGTAAAACGACGGCCAGTCCATATTGGAGTGGTTAGTCAAGA
NM_001163941_cds_13_0_chr7_20664654_f_1.fwd	TGTAAAACGACGGCCAGTAGCACCCAGAGGCTGAAGTA
NM_001163941_cds_14_0_chr7_20687653_f_1.fwd	TGTAAAACGACGGCCAGTTTTCTTAAACAGTGCAAAGGTTGT
NM_001163941_cds_15_0_chr7_20691844_f_1.fwd	TGTAAAACGACGGCCAGTGAAAGCTGTTCAGCAAGAACTACA
NM_001163941_cds_16_0_chr7_20704555_f_1.fwd	TGTAAAACGACGGCCAGTACAAATAGTCACTTGTGGCAAA
NM_001163941_cds_17_0_chr7_20705973_f_1.fwd	TGTAAAACGACGGCCAGTAAATTTTCACTTTTTCTGTTTCTTT
NM_001163941_cds_18_0_chr7_20706206_f.fwd	TGTAAAACGACGGCCAGTTGATATTCGTCATTTTGGGTGT
NM_001163941_cds_19_0_chr7_20710872_f.fwd	TGTAAAACGACGGCCAGTGGTGATGAGTAATGAGTCCAAGC
NM_001163941_cds_20_0_chr7_20729164_f_1.fwd	TGTAAAACGACGGCCAGTCTCAAAGTATAAATTCAAGGCATAAA
NM_001163941_cds_20_0_chr7_20729164_f_2.fwd	TGTAAAACGACGGCCAGTCAAAATGCAACTAACATGGGACT
NM_001163941_cds_21_0_chr7_20733188_f_2.fwd	TGTAAAACGACGGCCAGTGTGAGTGACTAGAATTCACAAATGG
NM_001163941_cds_22_0_chr7_20734463_f_1.fwd	TGTAAAACGACGGCCAGTGACCTTGCTATAATTCATGCCTCA
NM_001163941_cds_23_0_chr7_20745131_f_1.fwd	TGTAAAACGACGGCCAGTTGGTGGGTCTTCAGCGTTAG
NM_001163941_cds_23_0_chr7_20745131_f_2.fwd	TGTAAAACGACGGCCAGTGCTCGTTTTGGCTCCTGAAT
NM_001163941_cds_24_0_chr7_20749025_f_1.fwd	TGTAAAACGACGGCCAGTAACAAAAGTGACAGAAACCCACT
NM_001163941_cds_24_0_chr7_20749025_f_2.fwd	TGTAAAACGACGGCCAGTCAACCTTCCCAAGTCATTCTTC
NM_001163941_cds_25_0_chr7_20751380_f_1.fwd	TGTAAAACGACGGCCAGTTGAGCCTTCCTTGGGTAACT
NM_001163941_cds_25_0_chr7_20751380_f_2.fwd	TGTAAAACGACGGCCAGTAGCCTGTGCTCTTCAACTG
NM_001163941_cds_26_0_chr7_20759508_f_1.fwd	TGTAAAACGACGGCCAGTTGCAACAAAGCCCAAGAATA
NM_001163941_cds_27_0_chr7_20761575_f_1.fwd	TGTAAAACGACGGCCAGTGCAGTTCCTTTGGGGACAAG
NM_001163941_cds_27_0_chr7_20761575_f_2.fwd	TGTAAAACGACGGCCAGTTGGTCACTCACAGGCTCTCT
NM_001089_cds_0_0_chr16_2266676_r_1.fwd	TGTAAAACGACGGCCAGTCCAGCTCTGGGAAAGTGAAC
NM_001089_cds_1_0_chr16_2267599_r.fwd	TGTAAAACGACGGCCAGTCCCAAACCAGCACGTATCA
NM_001089_cds_2_0_chr16_2267881_r_1.fwd	TGTAAAACGACGGCCAGTATGCCTTGGTGCTCATCTT
NM_001089_cds_2_0_chr16_2267881_r_2.fwd	TGTAAAACGACGGCCAGTCAGATGGGAGAGGCCTAGGTA
NM_001089_cds_3_0_chr16_2268290_r_1.fwd	TGTAAAACGACGGCCAGTTCACACTCCTCCATGCTGTG
NM_001089_cds_3_0_chr16_2268290_r_2.fwd	TGTAAAACGACGGCCAGTACCCGGTGCTGAAACTTCC
NM_001089_cds_4_0_chr16_2268945_r_1.fwd	TGTAAAACGACGGCCAGTGGGCAGTCCCTTTCCTACG
NM_001089_cds_5_0_chr16_2271029_r_1.fwd	TGTAAAACGACGGCCAGTCATTACCTTGTCTCGCTGTCC
NM_001089_cds_5_0_chr16_2271029_r_2.fwd	TGTAAAACGACGGCCAGTCACCCACCTTTCCGACAT
NM_001089_cds_6_0_chr16_2271383_r_1.fwd	TGTAAAACGACGGCCAGTAGGCACCCAACAGAAAACAC
NM_001089_cds_7_0_chr16_2273188_r_1.fwd	TGTAAAACGACGGCCAGTGAGACCATCTGGTGCAGGA
NM_001089_cds_8_0_chr16_2274281_r_1.fwd	TGTAAAACGACGGCCAGTTGTGGTTCCTTGTTACAGATGC
NM_001089_cds_8_0_chr16_2274281_r_2.fwd	TGTAAAACGACGGCCAGTGGGACACTCACTATATTTCTTGCAGTA
NM_001089_cds_9_0_chr16_2274781_r_1.fwd	TGTAAAACGACGGCCAGTCTCTGCACAGGGCAAGGAC
NM_001089_cds_9_0_chr16_2274781_r_2.fwd	TGTAAAACGACGGCCAGTGAAGATGGTCAGCCTCGTGTA
NM_001089_cds_10_0_chr16_2275444_r_2.fwd	TGTAAAACGACGGCCAGTAGCTGGTTCCGGTTCTGC
NM_001089_cds_11_0_chr16_2276696_r_1.fwd	TGTAAAACGACGGCCAGTGTGGATGGTGGAGGAGGAT
NM_001089_cds_11_0_chr16_2276696_r_2.fwd	TGTAAAACGACGGCCAGTGCAGCTTGAACAGAAGGTTGT
NM_001089_cds_12_0_chr16_2278028_r_1.fwd	TGTAAAACGACGGCCAGTTCCAGGCATGTTTGATGGT
NM_001089_cds_12_0_chr16_2278028_r_3.fwd	TGTAAAACGACGGCCAGTGTACTCGCCCAAGGTCAGC
NM_001089_cds_13_0_chr16_2279436_r_2.fwd	TGTAAAACGACGGCCAGTCTCTGCATGGGCTTACATGA
NM_001089_cds_14_0_chr16_2282142_r_1.fwd	TGTAAAACGACGGCCAGTGCATTTACTGACCGAAGGAAGAC

(*continued*)

Supplementary Table S3. Continued

Sequence Name	Sequence
NM_001089_cds_15_0_chr16_2285592_r_1.fwd	TGTAAAACGACGGCCAGTACCCAGCCAAGCAGATTCAT
NM_001089_cds_16_0_chr16_2287331_r_1.fwd	TGTAAAACGACGGCCAGTGGCTGAACCACATCCTAACC
NM_001089_cds_16_0_chr16_2287331_r_2.fwd	TGTAAAACGACGGCCAGTCACCGCTCACCGTATTTCTG
NM_001089_cds_17_0_chr16_2287768_r_1.fwd	TGTAAAACGACGGCCAGTGGCTTGAGTCCTCCAAGGAT
NM_001089_cds_18_0_chr16_2288388_r_1.fwd	TGTAAAACGACGGCCAGTCCTTGACGTAGCTGGACTCA
NM_001089_cds_19_0_chr16_2289405_r_1.fwd	TGTAAAACGACGGCCAGTGCGCTGAGATGGTGTTAAAG
NM_001089_cds_20_0_chr16_2290007_r_1.fwd	TGTAAAACGACGGCCAGTAGGAGGGAGCAAGGCTCAG
NM_001089_cds_21_0_chr16_2293971_r_1.fwd	TGTAAAACGACGGCCAGTGCTCTGAAGCGGAAGGATTA
NM_001089_cds_21_0_chr16_2293971_r_2.fwd	TGTAAAACGACGGCCAGTAGAGCAGGGCATCAGAACTC
NM_001089_cds_22_0_chr16_2298452_r_1.fwd	TGTAAAACGACGGCCAGTAGCTATCCAGCCCACACTCA
NM_001089_cds_23_0_chr16_2307285_r_1.fwd	TGTAAAACGACGGCCAGTAGTCCAACCTTCCCCTGGT
NM_001089_cds_24_0_chr16_2307650_r_1.fwd	TGTAAAACGACGGCCAGTGGACATTGACAGCTCCTCTCC
NM_001089_cds_25_0_chr16_2309583_r_1.fwd	TGTAAAACGACGGCCAGTTACTAAAACACCAAGCCTTTGGA
NM_001089_cds_26_0_chr16_2313525_r_1.fwd	TGTAAAACGACGGCCAGTACCAAGCCAAATGTCCTGAA
NM_001089_cds_28_0_chr16_2316012_r_12.fwd	TGTAAAACGACGGCCAGTAGGTTTAAGGGAAAGCAGTG
NM_001089_cds_28_0_chr16_2316012_r_20.fwd	TGTAAAACGACGGCCAGTCCAAAGGAGAGACTGCTATTTACTC
NM_001089_cds_28_0_chr16_2316012_r_21.fwd	TGTAAAACGACGGCCAGTCATGTCTCACCTCGCATGTT
NM_001089_cds_29_0_chr16_2316415_r.fwd	TGTAAAACGACGGCCAGTGGGCACATTTTCCGACTG
Reverse primers	
NM_001163941_cds_1_0_chr7_20629434_f.rev	ACGATGAGAAATTCAGAAGAGGA
NM_001163941_cds_2_0_chr7_20632705_f.rev	GGATGTTATGCTATTTTTCCCTATC
NM_001163941_cds_3_0_chr7_20634836_f_1.rev	GCCCAGCAATATGGCAGAA
NM_001163941_cds_4_0_chr7_20638207_f.rev	CTCTGTCAACTACAACTCAAAGCATA
NM_001163941_cds_5_0_chr7_20649332_f_1.rev	CAAAGCTAACGTACTACAATATCATCC
NM_001163941_cds_6_0_chr7_20649609_f_1.rev	TGCATTAGCCATCTCACTTACC
NM_001163941_cds_6_0_chr7_20649609_f_2.rev	AAGGACATCATACTTTATCCATGC
NM_001163941_cds_7_0_chr7_20651904_f_1.rev	CCTTTGCATCTTTGAGATTCTG
NM_001163941_cds_8_0_chr7_20652109_f_1.rev	GAATTTTGGCTAAACTAGGTAAGGA
NM_001163941_cds_8_0_chr7_20652109_f_2.rev	CAAAAGCGGAATGCAGATG
NM_001163941_cds_9_0_chr7_20653683_f_1.rev	TTTCAATACAACACAATCTCCTCTT
NM_001163941_cds_10_0_chr7_20654116_f_1.rev	AGTTGATCCAGAGTTATTTGTCCA
NM_001163941_cds_11_0_chr7_20656170_f_1.rev	TATGGCTTCTCTCCCAGCTC
NM_001163941_cds_12_0_chr7_20657568_f_1.rev	TGCCACCATAAGCTAAGGACA
NM_001163941_cds_12_0_chr7_20657568_f_2.rev	GCCACATTGAAAGAAGAATTGTC
NM_001163941_cds_13_0_chr7_20664654_f_1.rev	CCATCACGTAAGTTCTCAGTGG
NM_001163941_cds_14_0_chr7_20687653_f_1.rev	TTGAAACACTCCATTTCTTTACTGA
NM_001163941_cds_15_0_chr7_20691844_f_1.rev	TGACACACTGATGCTAGAGTGAAA
NM_001163941_cds_16_0_chr7_20704555_f_1.rev	TCCCCTTGTGGTTTAGACTGA
NM_001163941_cds_17_0_chr7_20705973_f_1.rev	CTGACCTGATATAACATGGCTTTG
NM_001163941_cds_18_0_chr7_20706206_f.rev	GTCACACTTTTGGACTTGCTTCT
NM_001163941_cds_19_0_chr7_20710872_f.rev	ATGTGGGTCATCTCAGCACA
NM_001163941_cds_20_0_chr7_20729164_f_1.rev	CGATGGTGATAACAGTCTTCATTT
NM_001163941_cds_20_0_chr7_20729164_f_2.rev	TCTACCTTCTATCCTAAATTGGTCTGT
NM_001163941_cds_21_0_chr7_20733188_f_2.rev	TTTCAGGAAAATAAGAAAAATGTGC
NM_001163941_cds_22_0_chr7_20734463_f_1.rev	TCCATTTCCTGGGTTCAATC
NM_001163941_cds_23_0_chr7_20745131_f_1.rev	AGTGGCCCCCAGTTCCTACT
NM_001163941_cds_23_0_chr7_20745131_f_2.rev	TGACATTATCTTTTGCAGAGTTTTC
NM_001163941_cds_24_0_chr7_20749025_f_1.rev	AGGACTGCTAACCCCCAGAT
NM_001163941_cds_24_0_chr7_20749025_f_2.rev	TTGTGCTTCACTTCAGAGTCCT
NM_001163941_cds_25_0_chr7_20751380_f_1.rev	CTTAGCCTTACTTGGCAGCTTTA
NM_001163941_cds_25_0_chr7_20751380_f_2.rev	GGTCGTAGGAAAATCGTCACA
NM_001163941_cds_26_0_chr7_20759508_f_1.rev	AGCCTTAATTGGAACTGGTGA
NM_001163941_cds_27_0_chr7_20761575_f_1.rev	CCTTCTTTGCATTACACGAACA
NM_001163941_cds_27_0_chr7_20761575_f_2.rev	GCAGAAGTTGATGGGAAATAAA
NM_001089_cds_0_0_chr16_2266676_r_1.rev	GCCAGAGGACTCCCAGGT
NM_001089_cds_1_0_chr16_2267599_r.rev	CTGTGCGGAGCGTCTGTG
NM_001089_cds_2_0_chr16_2267881_r_1.rev	CACAGCATGGAGGAGTGTGA
NM_001089_cds_2_0_chr16_2267881_r_2.rev	CAGGAGACCCATCAGCATCT

(*continued*)

Supplementary Table S3. Continued

Sequence Name	Sequence
NM_001089_cds_3_0_chr16_2268290_r_1.rev	CAGCCTTATTCCCCCACCT
NM_001089_cds_3_0_chr16_2268290_r_2.rev	GCAGATGTCTTCCCATGTAGG
NM_001089_cds_4_0_chr16_2268945_r_1.rev	GGTAGTCCCCGTGGTCCT
NM_001089_cds_5_0_chr16_2271029_r_1.rev	TGCTCTGCTTTGCGTCCA
NM_001089_cds_5_0_chr16_2271029_r_2.rev	AGATGTAGCGGACGAGAGGA
NM_001089_cds_6_0_chr16_2271383_r_1.rev	GTCTGAGTCGCACCTGTGG
NM_001089_cds_7_0_chr16_2273188_r_1.rev	GCTGTGACCTACTGGCCTTC
NM_001089_cds_8_0_chr16_2274281_r_1.rev	TCCAGCGCAGACTGATCTTA
NM_001089_cds_8_0_chr16_2274281_r_2.rev	GGCCCAGTTCATGCTCAC
NM_001089_cds_9_0_chr16_2274781_r_1.rev	GCCGCAGGTGGTGTTTAAG
NM_001089_cds_9_0_chr16_2274781_r_2.rev	TGCACCCTCAGCCTTTACC
NM_001089_cds_10_0_chr16_2275444_r_2.rev	CATGGTGCTTGTGCTCTCC
NM_001089_cds_11_0_chr16_2276696_r_1.rev	GTGACCTGGAGGAGTTCTTGA
NM_001089_cds_11_0_chr16_2276696_r_2.rev	CAGCTCCTTTCCCGGTTC
NM_001089_cds_12_0_chr16_2278028_r_1.rev	GCGCGAGTGGAAAATGGT
NM_001089_cds_12_0_chr16_2278028_r_3.rev	AAAATAGTGCCAACGTGCAG
NM_001089_cds_13_0_chr16_2279436_r_2.rev	ATGGTGGCCGGAGACACT
NM_001089_cds_14_0_chr16_2282142_r_1.rev	GTTCAAGTGTTCTCCTGCCTCT
NM_001089_cds_15_0_chr16_2285592_r_1.rev	CTCCGGTTCTCTAGCCTCCT
NM_001089_cds_16_0_chr16_2287331_r_1.rev	TCCCTCCAGGTGCTGATACT
NM_001089_cds_16_0_chr16_2287331_r_2.rev	GACTGGAGGCAGTGGGTTC
NM_001089_cds_17_0_chr16_2287768_r_1.rev	CCTCTCACCAGAACCTTGCT
NM_001089_cds_18_0_chr16_2288388_r_1.rev	CAGTGGGAGTGGGGTTCC
NM_001089_cds_19_0_chr16_2289405_r_1.rev	AGGGTGTCTGGGACGTGTT
NM_001089_cds_20_0_chr16_2290007_r_1.rev	CCTTCACAGGGATGAAACAAG
NM_001089_cds_21_0_chr16_2293971_r_1.rev	GGCCACTTTCCTGATGTGTC
NM_001089_cds_21_0_chr16_2293971_r_2.rev	TGAATGAGCTGTTGCTGGTC
NM_001089_cds_22_0_chr16_2298452_r_1.rev	GTAGGGGGTTGCCTGTACCT
NM_001089_cds_23_0_chr16_2307285_r_1.rev	TTTGTGGTCAGAGACTTCAGAGA
NM_001089_cds_24_0_chr16_2307650_r_1.rev	CAGGAGTTTGAGCAAGATGAG
NM_001089_cds_25_0_chr16_2309583_r_1.rev	CATCTCTTCCCCCATGGAC
NM_001089_cds_26_0_chr16_2313525_r_1.rev	CGGGGGAGTGGTGAGTTCT
NM_001089_cds_28_0_chr16_2316012_r_12.rev	GCTCTGACCCTGCCATTCT
NM_001089_cds_28_0_chr16_2316012_r_20.rev	CCTGCCATTGCTGTTTTCTG
NM_001089_cds_28_0_chr16_2316012_r_21.rev	CCTCCTCTGGAAGAACTACACC